

# Habitat-adapted microbial communities mediate *Sphagnum* peatmoss resilience to warming

Alyssa A. Carrell<sup>1\*</sup> , Travis J. Lawrence<sup>1\*</sup> , Kristine Grace M. Cabugao<sup>2</sup> , Dana L. Carper<sup>1</sup> , Dale A. Pelletier<sup>1</sup> , Jun Hyung Lee<sup>1</sup> , Sara S. Jawdy<sup>1</sup> , Jane Grimwood<sup>3,4</sup> , Jeremy Schmutz<sup>3,4</sup> , Paul J. Hanson<sup>5</sup> , A. Jonathan Shaw<sup>6</sup>  and David J. Weston<sup>1</sup> 

<sup>1</sup>Biosciences Division, Oak Ridge National Laboratory, 1 Bethel Valley Rd, Oak Ridge, TN 37831, USA; <sup>2</sup>Bredesen Center for Interdisciplinary Research and Graduate Education, University of Tennessee, 1502 Cumberland Ave., Knoxville, TN 37996, USA; <sup>3</sup>HudsonAlpha Institute for Biotechnology, 601 Genome Way, Huntsville, AL 35806, USA; <sup>4</sup>Department of Energy Joint Genome Institute, Lawrence Berkeley National Lab, 1 Cyclotron Rd., Berkeley, CA 94720, USA; <sup>5</sup>Environmental Sciences Division, Oak Ridge National Laboratory, 1 Bethel Valley Rd, Oak Ridge, TN 37831, USA; <sup>6</sup>Duke University, 2127 Campus Drive, Durham, NC 27708, USA

## Summary

Author for correspondence:  
David J. Weston  
Email: westondj@ornl.gov

Received: 25 June 2021  
Accepted: 21 February 2022

New Phytologist (2022) 234: 2111–2125  
doi: 10.1111/nph.18072

**Key words:** climate change, heat tolerance, microbiome transfer, moss, peatland, *Sphagnum*, symbiosis, synthetic communities.

- *Sphagnum* peatmosses are fundamental members of peatland ecosystems, where they contribute to the uptake and long-term storage of atmospheric carbon. Warming threatens *Sphagnum* mosses and is known to alter the composition of their associated microbiome. Here, we use a microbiome transfer approach to test if microbiome thermal origin influences host plant thermotolerance.
- We leveraged an experimental whole-ecosystem warming study to collect field-grown *Sphagnum*, mechanically separate the associated microbiome and then transfer onto germ-free laboratory *Sphagnum* for temperature experiments. Host and microbiome dynamics were assessed with growth analysis, Chla fluorescence imaging, metagenomics, metatranscriptomics and 16S rDNA profiling.
- Microbiomes originating from warming field conditions imparted enhanced thermotolerance and growth recovery at elevated temperatures. Metagenome and metatranscriptome analyses revealed that warming altered microbial community structure in a manner that induced the plant heat shock response, especially the HSP70 family and jasmonic acid production. The heat shock response was induced even without warming treatment in the laboratory, suggesting that the warm-microbiome isolated from the field provided the host plant with thermal preconditioning.
- Our results demonstrate that microbes, which respond rapidly to temperature alterations, can play key roles in host plant growth response to rapidly changing environments.

## Introduction

*Sphagnum* peat mosses are fundamental ecosystem engineers (Clymo & Hayward, 1982; van Breemen *et al.*, 1995), contributing to the construction of bog and peatland systems that occupy just 3% of the global land surface yet store *c.* 30% of all soil carbon (Gorham, 1991; Yu *et al.*, 2010). In boreal regions, *Sphagnum* production can increase with modest warming (Robroek *et al.*, 2007b; Hupperts *et al.*, 2021), but these positive effects are not entirely generalizable (Gunnarsson *et al.*, 2004) and are expected to be offset by water stress from surface drying (Robroek *et al.*, 2007a) and more extreme warming events in the future (Bragazza, 2008; Bragazza *et al.*, 2016; Norby *et al.*, 2019). The competitive success and productivity of this keystone genus is largely dependent on symbiotic interactions with microbial

associates (Lindo *et al.*, 2013; Weston *et al.*, 2014; Kostka *et al.*, 2016), through which *c.* 35% of atmospheric nitrogen fixed by diazotrophic bacteria in the microbiome is transferred to the *Sphagnum* host (Berg *et al.*, 2013). Currently, however, we lack a basic understanding of how warming influences *Sphagnum*–microbiome interactions and how these interactions influence host acclimation and adaptation to elevated temperature.

*Sphagnum* symbiosis is characterized by an intimate association with dinitrogen (N<sub>2</sub>)-fixing cyanobacteria on the host cell surface and within water-filled hyaline cells (Granhall & Hofsten, 1976; Basilier *et al.*, 1978; Basilier, 1979, 1980). Hyaline cells help nonvascular mosses retain water and also provide a buffered environment for the microbiome that is less harsh than the external pore water, which is characterized by fluctuating temperature spikes and low pH (Clymo & Hayward, 1982). Phylogenetic evidence suggests that bacterial methanotrophs are also important N<sub>2</sub>-fixing members of the *Sphagnum* microbiome in boreal

\*These authors contributed equally to this work.

peat bogs (Kip *et al.*, 2010; Liebner & Svenning, 2013; Larmoia *et al.*, 2014; Vile *et al.*, 2014). These methanotrophs not only fix N<sub>2</sub> but also supply 5–20% of the CO<sub>2</sub> necessary for host photosynthesis as a byproduct of methane oxidation (Raghoebarsing *et al.*, 2005). In addition to the prominent N<sub>2</sub>-fixing bacteria, *Sphagnum* spp. host a diverse array of heterotrophic bacteria, archaea (Kostka *et al.*, 2016), fungi (Kostka *et al.*, 2016), protists (Lamentowicz & Mitchell, 2005; Jassey *et al.*, 2015) and viral symbionts (Stough *et al.*, 2018) within a complex food web structure. Results from a whole ecosystem peatland warming experiment indicate that elevated temperatures are associated with changes in the *Sphagnum* microbial biomass (Basińska *et al.*, 2020), microbial community (Carrell *et al.*, 2019; Reczuga *et al.*, 2020), reduced N<sub>2</sub> fixation (Carrell *et al.*, 2019) and reduced *Sphagnum* biomass production (Norby *et al.*, 2019). It remains unknown whether the warming-altered microbiome influences host acclimation, growth and production, and if so, in what manner.

Disentangling the effects of *Sphagnum* symbiotic interactions in the context of climate change is complicated by our inability to predict whether and how mutually beneficial interactions will persist under variable environments. In N<sub>2</sub>-fixing legumes (Heath *et al.*, 2010) and coral systems (Cunning *et al.*, 2015; Bay *et al.*, 2016; Howells *et al.*, 2016; Baker *et al.*, 2018), for example, altered environmental conditions can increase the cost of the interaction relative to the benefits (i.e. the cost:benefit ratio), resulting in breakdown of mutualism and can even lead to antagonistic interactions. One strategy for maintaining a favorable cost:benefit ratio is partner switching, that is the substitution of one symbiont for another. In corals, for example, the negative effect of elevated temperatures on host performance can be tempered by replacing symbiont partners with more thermotolerant species (Bay *et al.*, 2016; Howells *et al.*, 2016). Another strategy is the habitat-adapted symbiosis paradigm that does not emphasize partner choice, but instead proposes that endophytes adapt to stress in a habitat-specific manner and can confer the same functional stress tolerance to their plant hosts (Rodriguez *et al.*, 2008). Because it is not known whether endophytes are locally adapted or differentiated by environmental sorting, the term 'adaptation' is applied loosely (Giauque *et al.*, 2019). Nonetheless, habitat-associated benefits from endophytes originating from extreme temperatures and salinities can benefit host plants subjected to the same environmental extremes (Redman *et al.*, 2011). By contrast, the habitat origin of fungal endophytes along a rainfall gradient had little effect on the drought responses of *Panicum virgatum* (Giauque & Hawkes, 2013). A more explicit test of habitat-associated effects relative to evolutionary history and physiological traits was carried out by Giauque *et al.* (2019). They found little support for the idea that fungal endophyte phylogenetic relatedness predicts host benefits, but did find some evidence that microbes that had experienced similarly stressful environments could benefit their hosts. However, the host benefit was not as strong as in previous studies (Rodriguez *et al.*, 2008), in which fungal endophytes were isolated from more extreme environments. Further complicating the habitat-adaptation

paradigm is our lack of understanding of the underlying mechanism in conferring host benefits.

Given the importance of bacteria for *Sphagnum* performance and ecosystem biogeochemistry (Raghoebarsing *et al.*, 2005; Kip *et al.*, 2010; Lindo *et al.*, 2013; Kostka *et al.*, 2016), we sought to determine the influence of habitat origin on host acclimation to thermal stress. To investigate this experimentally, we mechanically separated the microbiome from field-grown *Sphagnum* plants collected under an ambient and a warm condition, transferred the constituent microbes to axenic plants, and then exposed the new host plants to short-term heat stress. To assess host and bacterial dynamics, we performed growth analysis, Chl<sub>a</sub> fluorescence imaging, metagenomics, metatranscriptomics and 16S rDNA profiling. The transfer of environmentally conditioned microbiomes to axenic plants, which is analogous to microbiome transplant studies in medical research, allowed us to test the following hypotheses: the isolation and transfer of a microbiome adapted to a warming origin can transmit thermotolerance to the plant host, the warming environment selects for microbial symbionts that can maintain nitrogen transfer with the plant at elevated temperatures, and the warming-adapted microbiome elicits a host gene response enriched in nitrogen metabolism and abiotic stress response.

## Materials and Methods

### Study site and field sampling

The Spruce and Peatland Responses Under Changing Environments (SPRUCE) experiment, located in the S1 bog of the Marcell Experimental Forest (47°30.4760'N, 93°27.1620'W; 418 m above mean sea level), MN, USA, uses a regression-based design at the whole-ecosystem scale to produce nominal warming of ambient +0, +2.25, +4.5, +6.75 and +9°C in a *Picea mariana*–*Sphagnum* spp. raised bog ecosystem with open-top chamber systems (Hanson *et al.*, 2016). Heating of the soil was initiated in June 2014 and aboveground air heating began in June 2015. A full discussion of the experimental details and ecosystem description is available (Hanson *et al.*, 2016). To obtain field-conditioned microbiomes, 100 g of living green stems of fully hydrated, hollow dwelling *Sphagnum angustifolium* (Russow) C.E.O. Jensen was collected from ambient +0°C (ambient) and ambient +9°C (elevated) plots in August 2016 and August 2017. The collected stem portion typically included capitula and 2–3 cm of living stem. The *Sphagnum* material of each microbiome was placed in an individual sterile bag and shipped to Oak Ridge National Laboratory on blue ice.

### Microbiome transfer to axenic *Sphagnum* and warming treatment

To isolate the microbiomes from each field-conditioned microbiome, a sample of 100 g of tissue was diced with a sterile razor blade and pulverized in PBS with a mortar and pestle. The resulting suspension was filtered through Mira Cloth, centrifuged to pellet the microbes, and then resuspended in 500 ml

BG11 -N medium (pH 5.5). Glycerol stocks of 100 ml of inoculum were frozen and stored at  $-80^{\circ}\text{C}$ . Axenic tissue-culture *Sphagnum* was propagated via clonal shoot propagation of *Sphagnum* generated from ethanol sterilized *Sphagnum* spores collected from the S1 bog. A single capitulum of axenic *S. angustifolium* was added to each well of a 12-well plate and inoculated with 2 ml of ambient-microbiome, warm-microbiome or sterile media. The repeated 2017 experiment used the same experimental design, except that the number of replicate plants was increased from  $n=6$  to  $n=12$ . The *Sphagnum angustifolium* genotype was the same as that sequenced by the DOE JGI ([https://phytozome-next.jgi.doe.gov/info/Sfallax\\_v1\\_1](https://phytozome-next.jgi.doe.gov/info/Sfallax_v1_1)). The sealed plates were placed into growth chambers with a  $350\ \mu\text{mol m}^{-2}\ \text{s}^{-1}$  of photosynthetically active radiation (PAR), 12 h : 12 h, light : dark cycle, programmed to either ambient or elevated field plot temperatures. August 2016 field plot temperatures from 6 h blocks were averaged from each day, resulting in a cycle of four temperatures. August 2017 temperatures did not differ from those in August 2016, so the same temperature profile was used for incubations for both years (Supporting Information Table S1). The plates were randomly distributed throughout the reach-in growth chamber and positions were randomly shuffled weekly to account for possible edge effects or light variation across the chamber. Sufficient RNA could not be isolated from all treatments in 2016 so the incubation duration of the 2016 experiment was reduced from 4 to 3 wk in the 2017 experiment.

To determine if the growth response of inoculated *Sphagnum* resulted from residual plant molecules or the microbiome obtained during the isolation of thermal-origin microbiomes, we repeated the experiment with a heat-killed microbial control from glycerol stocks of the thermal-origin microbiomes. Glycerol stocks were thawed, microbes were pelleted via centrifugation, rinsed and resuspended in BG11 -N, and an aliquot of glycerol stock was heat-killed. Each microbiome, heat-killed control or no microbial control were applied to axenic *S. angustifolium* and placed in growth chambers for temperature treatments (Table S1).

### Measurement of growth and photosynthesis

To measure growth, images from the top of each plate were collected weekly, and surface area was measured using the IMAGEJ software (Schneider *et al.*, 2012). The change in surface area was determined as a proxy for growth (Heck *et al.*, 2021). To estimate maximal photosystem II (PSII) quantum yield, Chl fluorescence parameters were measured weekly with a FluorCam FC800 (PSI, Bruno, Czech Republic) after 20 min of dark adaptation. Maximum quantum yield (QY<sub>max</sub>) was determined using the FLUORCAM 7 software.

Normality of the data was checked using the Shapiro–Wilk test before checking homoskedasticity of variances using Levene's test in the R package CAR (Fox & Weisberg, 2018). Growth rate ( $\text{mm d}^{-1}$ ) and total growth over the duration of the experiment were rank-transformed before two-way ANOVA to assess the influence of experimental temperature and donor microbiome.

Fluorescence ( $F_v/F_m$ ) was measured in moss as a proxy for photosynthetic activity throughout the experiment. However, to highlight the greatest differences in donor microbiome and experimental temperature combinations, only fluorescence data from the last week were used. Fluorescence data were also rank-transformed before using a two-way ANOVA.  $\alpha = 0.05$  was used to denote statistical significance in both two-way ANOVA and Tukey's honest significant difference (HSD) *post hoc* analyses. Growth and fluorescence statistics were analyzed using R v.3.5.1 (R Core Team, 2021).

### 16S rDNA and ITS sequencing of community profiles

To characterize bacterial/archaeal and fungal components of the microbiomes of inocula and final microbiomes of the laboratory experiments, each sample ( $n=3$  for inocula and  $n=5$  for laboratory experiments) was pulverized in liquid  $\text{N}_2$ , and DNA was extracted from 50 mg of material using the DNeasy PowerPlant Pro Kit (Qiagen). Extracted DNA was taken to the Genomics Core at the University of Tennessee, Knoxville, TN, USA, for library preparation and sequencing on an Illumina MiSeq (San Diego, CA, USA). Libraries were prepped for the 16S rRNA gene by means of a two-step PCR approach with a mixture of custom 515F and 806R primers (Cregger *et al.*, 2018) to characterize archaeal/bacterial communities, and for the ITS2 gene region with a custom mixture of primers to characterize the fungal community. Samples were pooled in equal concentrations and sequenced on the MiSeq with negative control samples.

Microbial sequences were processed with the QIIME 2 v.2018.11 platform (Bolyen *et al.*, 2019). Paired sequences were demultiplexed with the plugin demux and quality-filtered (denoised, dereplicated, chimera-filtered and pair-end merged) and processed into sequence variants (SVs) with the DADA2 plugin (Callahan *et al.*, 2016). Taxonomy was assigned using a pre-trained Naive Bayes classifier based on the Greengenes v.13\_8 database (99% operational taxonomic units (OTUs)) that are trimmed to the 515F/806R primer pair for 16S rDNA and based on the UNITE database (99% OTUs) for ITS2. Sequences assigned as chloroplast or mitochondria were removed. Microbial diversity was calculated based on a subsample of 19 000 sequences to fit the size of the smallest library. SV-based alpha diversity (Shannon diversity) and beta diversity (Bray–Curtis) were calculated using the PHYLOSEQ 1.30.0 (McMurdie & Holmes, 2013) package in R (R Core Team, 2021). Beta diversity was visualized using nonmetric multidimensional scaling ordination (NMDS) based on Bray–Curtis similarity distances. A permutational multivariate analysis of variance (PERMANOVA) with 999 permutations was used to calculate the significance of clustering of samples by microbial and chamber treatment. The correlation between microbial diversity and *Sphagnum* growth was assessed using Pearson correlation.

### Metatranscriptomics profiling

Only 2017 experimental samples were profiled for metatranscriptomics as sufficient RNA could not be isolated from

2016 experimental samples. Cryogenically stored samples from the end of the experiment were ground in liquid nitrogen, and total RNA was extracted using a method combining CTAB lysis buffer and the Spectrum Total Plant RNA extraction kit (Sigma) as described previously (Timm *et al.*, 2016). RNA quality and quantity were determined using a NanoDrop Spectrophotometer (Thermo Scientific, Waltham, MA, USA). Total RNA (3 µg) of three biological replicates was sent to Macrogen (Seoul, South Korea), where libraries were prepared with TruSeq Stranded RNA with Ribo-Zero-Plant and sequenced on an Illumina HiSeq 2500 in Rapid Run mode (paired-end, 2 × 150 nt).

Metatranscriptome reads were partitioned into *S. angustifolium* and microbial transcripts by mapping reads to the *S. angustifolium* v.1.0 genome using BBMAP v.38.22. Microbial transcripts were processed using the SAMSA v.2.2.0 pipeline (Westreich *et al.*, 2016), except that differentially expressed SEED functional gene ontologies (Overbeek *et al.*, 2014) were identified using LIMMA-VOOM v.3.11 (Ritchie *et al.*, 2015) with multiple testing correction using false discovery rate (FDR). Taxonomic classification of microbial transcripts was performed by mapping reads to the metagenome assembly using BAMM v.1.7.3 and transferring the taxonomic classification of metagenomic gene models and metagenome-assembled genome (MAG) assignments to mapped transcripts.

To identify differentially expressed (DE) *S. angustifolium* genes, *S. angustifolium* read-pairs were mapped to the *S. angustifolium* v1.0 reference genome using RSUBREAD v.2.3.0 (Liao *et al.*, 2019) and analyzed using LIMMA-VOOM v.3.11. Enrichment of MAPMAN4 ontology bins (Schwacke *et al.*, 2019) in the set of DE genes was determined using the MAPMAN desktop application v.3.6.0RC1 (Thimm *et al.*, 2014). The statistical significance of MAPMAN ontology bins was determined using a Kruskal–Wallis test with multiple testing correction using FDR in R v.3.6.1. The log<sub>2</sub>(fold change) (LFC) of MAPMAN4 ontology bins was determined by averaging LFC across DE genes within each bin. For all analyses we used a FDR-corrected *P*-value < 0.05 to determine statistically significant results.

### Metagenomics of the starting inoculum and phylogenetic analysis of cyanobacterial MAGs

A composite ambient-microbiome and a composite warming-microbiome sample were sequenced as an Illumina TruSeq PCR-Free library on an Illumina 2500 in Rapid Run mode (paired-end, 2 × 150 nt). Full details are provided in Methods S1.

## Results

### Plant host performance in response to experimental temperature is dependent on the thermal origin of the microbiome

In both years, a donor microbiome that matched the experimental thermal conditions conferred the greatest increase in host growth (Fig. 1b). Host benefits from the microbiome were

especially apparent under experimental warming conditions: in 2016 and 2017, moss receiving a warm-microbiome exhibited an increase in growth of 89 and 87%, respectively, relative to plants receiving the mock control (Fig. 1b; Tables S2–S4). By contrast, under experimental warming conditions moss inoculated with a temperature-mismatched microbiome (i.e. receiving ambient-microbiome and warming treatment) did not perform statistically significantly better than moss without a microbiome (Table S4), indicating that a microbiome preadapted to warming conditions specifically is conferring a growth advantage in the warming chamber. Host benefits from temperature-mismatched microbiomes were least prominent under ambient experimental treatment, in which growth increases ranged from 3% to 17% following inclusion of a warm-microbiome ( $F_{\text{temperature} : \text{microbiome}} = 32.01$ ;  $P < 0.05$  for 2017; Table S3). Throughout the experiment, moss photosynthetic activity and response to temperature and microbiome origin were evaluated by monitoring Chl*a* fluorescence ( $F_v/F_m$ ). The results mirrored the growth analysis:  $F_v/F_m$  values were 11–45% higher when microbiome thermal origin matched experimental temperature (Tables S5, S6; Figs S1, S2).

To test the viability of the contribution of the conditioned microbiome and molecules collected during inoculum isolation, we repeated the conditioned microbiome experiment with glycerol stocks of +0°C and +9°C microbiomes collected from the SPRUCE field site. Moss phenotypes of heat-killed controls were consistent with no microbe controls ( $P > 0.99$ ) while growth rates were highest in temperature-matched microbiome treatments and lower in discordant microbiome treatments (Fig. S3). Hence, the thermal tolerance conferred by the microbial inoculums is from direct contact with living organisms, and not an indirect consequence or nutrients, signaling compounds or other molecules acquired during isolation.

### Habitat origin and thermal treatment conditions structure the starting microbiome and resultant microbial community

Amplicon sequencing produced an average of 83 847 ± 53 040 reads after quality filtering (Table S7). In the 2016 inoculum, we retained 82% of the ambient-microbiome SVs and 85% of the warm-microbiome SVs compared to the unprocessed field-microbiome. In 2017, the ambient-microbiome and warm-microbiome represented 76 and 89% respectively of the SVs identified in the field-microbiomes. Across the treatments, we recovered an average of 482 SVs with an average of 350 bacterial/archaeal SVs and an average of 107 fungal SVs. In 2017, the initial community structure of the *S. angustifolium* field-collected inoculum differed between thermal origins (Adonis,  $R^2 = 0.92133$ ,  $P = 0.009$ ) and 2016 (Adonis,  $R^2 = 0.53$ ,  $P = 0.1$ ) (Fig. S4). The bacterial phylum Proteobacteria dominated all reads (21–68%) with cyanobacteria increasing in abundance in 2017 (15%) compared to 2016 (3%) (Fig. 1c). At the class level, the ambient-microbiome consisted largely of Alphaproteobacteria (32%) and Clostridia (16%) in 2016, whereas Alphaproteobacteria (30%) and Acidobacteria (11%) were most abundant in 2017 (Table S8). Within the warm-microbiome,

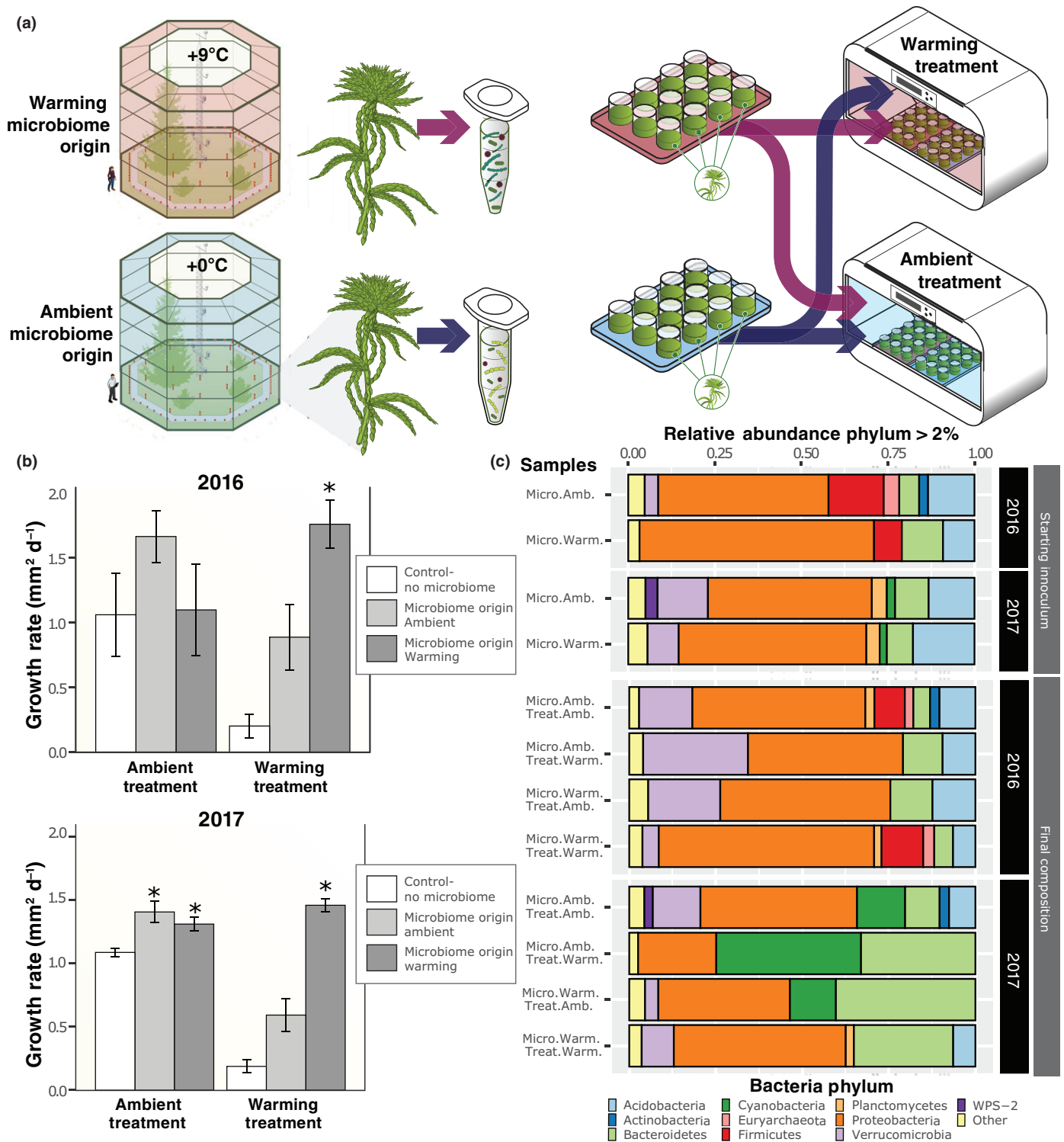


**Fig. 1** (a) Experimental approach and design: field-collected donor moss microbiomes collected from ambient or warming conditions were transferred to germ-free recipient moss (*Spangium angustifolium*), and the resulting communities were then placed in an ambient or warm growth chamber. (b) Average moss growth rate under ambient or warming treatments, as a function of the thermal origin of the microbiome. Error bars represent standard error of the mean of  $n = 6$  for 2016,  $n = 12$  for 2017. (c) Relative abundance of microbiome phyla, determined by 16S rDNA amplicon sequencing of the starting field-collected inoculum ( $n = 3$  of each composite sample) from ambient or warming experimental plots, and the final compositions of experimental samples ( $n = 6$  for each condition). An asterisk indicates statistical significance ( $P < 0.05$ ) based on a Tukey's HSD *post hoc* test of the percentage change of total growth between moss with a microbiome and moss without a microbiome within the same chamber.

Gammaproteobacteria were highly abundant in 2016 (43%), but only constituted 15% of the community abundance in 2017, with the difference compensated for by an additional increase in Alphaproteobacteria abundance (30%). Despite between-year differences in community composition at the class level within thermal regimes, the growth benefits provided to the plant were strikingly consistent (Fig. 1b).

*Sphagnum*-associated microbial communities responded to 4 wk of thermal treatment conditions regardless of year, thermal origin or growth temperature. NMDS ordinations of the microbiome Bray–Curtis distance matrix revealed that the community composition of the warm-microbiomes responded similarly across thermal treatments, whereas ambient-microbiome structure varied to a greater extent both across and within thermal treatments (Fig. S5). To determine whether changing community structure influenced microbial diversity, we estimated the Shannon diversity index for each treatment condition at the conclusion of the study in both years (Fig. 2a,b). Microbial Shannon diversity was highest when microbiome thermal origin matched chamber treatment temperatures; conversely, discordant combinations resulted in substantially lower microbial Shannon diversity (Fig. 2a,b). The ambient-microbiome had the highest diversity under matched (i.e. ambient) treatment conditions in both years (ANOVA,  $P < 0.01$ ). Similarly, the warm-origin microbiome had the highest diversity under the warming treatment in both years (ANOVA,  $P < 0.01$ ). Detailed class-level community composition assignments are provided in Table S9. Given that greater phylogenetic diversity is likely to be accompanied by greater metabolic and functional diversity, we expected that microbial diversity would be associated with enhancements in plant acclimation to stressful warming conditions, reflected by improved growth. As expected, bacterial and archaea Shannon diversity (as inferred from 16S rDNA) at the end of the

experiment was correlated with *Sphagnum* growth (Pearson correlation,  $r = 0.744$ ,  $P = 0.003$ ; Fig. 2b). By contrast, ITS-derived fungal Shannon diversity estimates did not correlate with moss growth (Pearson correlation,  $r = -0.204$ ,  $P = 0.403$ ; Fig. S6). The fungal communities did not vary greatly across treatments with the identification of just one phylum level (Table S10), three class levels (Table S11), and RNA sequencing (RNA-seq) reads that only constituted 0.6% of the total (Tables S12), so we largely focus on the bacterial component of the microbiome in the following sections.

### Metagenome and metatranscriptome analyses reveal changes in symbiotic microbe abundance and composition in response to thermal origin and temperature treatment

Host thermal acclimation and productivity varied with microbiome origin. To further explore how community dynamics influence host thermal acclimation, we used metagenomics and metatranscriptomics to identify both plant and microbial gene sets responsive to thermal and microbiome conditions (Fig. 3). For metagenome assemblies, DNA sequencing reads mapping to the *S. angustifolium* genome ([https://phytozome-next.jgi.doe.gov/info/Sfallax\\_v1\\_1](https://phytozome-next.jgi.doe.gov/info/Sfallax_v1_1)) were removed, and the remaining reads were coassembled into 4 762 069 contigs with an N50 of 1261 bp. Binning of metagenome contigs yielded 45 MAGs with a quality score  $\geq 70$  with  $\leq 5\%$  contamination (Table S12). The high-quality MAG standard of  $> 90\%$  complete and  $< 5\%$  contamination (Bowers *et al.*, 2017) was met for 28 of our genomes, whereas 13 and nine MAGs are  $> 95\%$  and  $> 97\%$  complete, respectively. Taxonomic assignments and BLAST hits from annotated proteins were resolved to the lowest taxonomic level using CHECKM (Parks *et al.*, 2015) and DIAMOND (Buchfink *et al.*, 2014) (Table S12). For metatranscriptomes, we generated

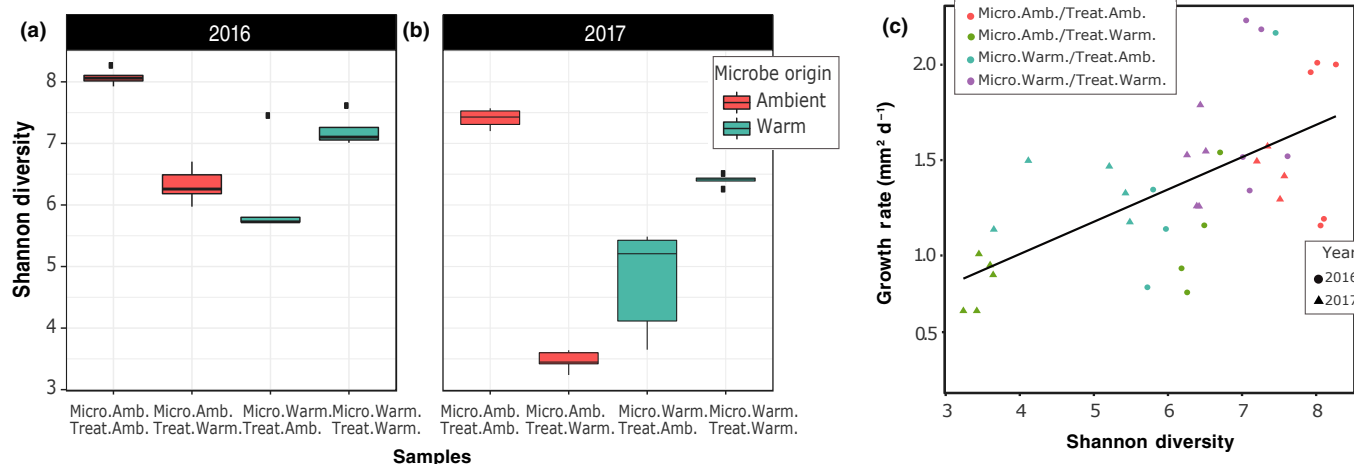


**Fig. 2** Microbial diversity change in response to habitat origin and experimental temperature. Shannon diversity index of the microbiome at the conclusion of the experiments in 2016 (a) and 2017 (b), based on 16S rDNA amplicon data for five replicates of each condition in each year. Microbiomes had lower Shannon diversity when the thermal origin and experimental treatment were mismatched (i.e. ambient origin in warming treatment or warming origin in ambient treatment) (ANOVA,  $P < 0.01$ ). Lines within the boxplots represent median, 25<sup>th</sup> and 75<sup>th</sup> percentile values, while whiskers are defined by the largest value not greater than  $1.5 \times$  the interquartile range (IQR) and the smallest value not less than  $1.5 \times$  the IQR. (c) *Sphagnum angustifolium* growth rate was linearly correlated with microbiome Shannon diversity (Pearson correlation,  $r = 0.744$ ,  $P = 0.003$ ) at the conclusion of the experiment.

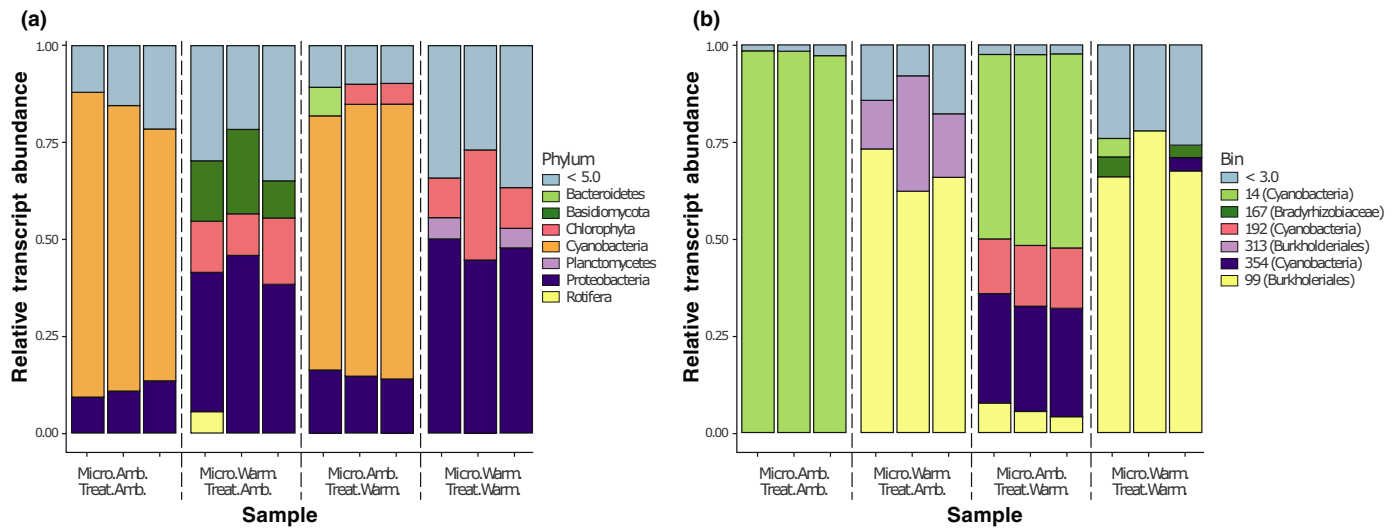


**Fig. 3** Microbial community transcriptional profile response to temperature treatment. Relative abundance of microbial transcripts mapping to metagenome contigs for (a) major phyla and (b) metagenome-assembled genomes (MAGs). Each bar represents a metatranscriptome sample for the ambient-microbiome (Micro. Amb.) or warming-microbiome (Micro. Warm) under either the ambient (Treat. Amb.) or warming (Treat. Warm) treatment. Colors indicate (a) phyla or (b) MAGs; light blue represents (a) phyla with < 5% of mapped transcripts or (b) MAGs with < 3% of mapped transcripts.

429.6 GB of RNA-seq data across three replicates for each treatment. On average,  $40.93 \pm 7.39$  million reads passed quality filtering per sample across all thermal treatments and microbiome conditions (Table S13). In samples derived from plants receiving a microbiome transfer, *c.* 65% of reads aligned to the *Sphagnum* genome, except in the discordant case when plants received ambient-microbiome followed by warming treatment. Under that condition, the plants were severely stressed, and only 12.4% of the reads aligned to the *Sphagnum* genome (Fig. S7).

To expand on the amplicon-based community composition results (Fig. 1c; Table S8) and determine which microbial members are transcriptionally active, we categorized transcriptional profiles based on taxonomic composition. Under matched ambient origin and experimental temperature, microbial transcripts were mostly from Cyanobacteria symbionts ( $72.5 \pm 6.9\%$ ), followed by Proteobacteria ( $11.2 \pm 2.2\%$ ) (Fig. 3a). Under matched warm-microbiome and warm-temperature treatment, Cyanobacteria transcript reads were largely absent, and the metatranscriptome was mainly derived from Proteobacteria ( $47.5 \pm 2.7\%$ ), Chlorophyta ( $16.39 \pm 10.4\%$ ) and Planctomycetes ( $4.9 \pm 0.57\%$ ). Results from mismatched origin and experimental conditions more closely reflected their microbiome origin communities (Table S8). This finding was also reflected in a multidimensional scaling analysis using level 3 SEED functional annotation, in which cluster variation was explained more based on microbial origin rather than experimental temperature (Fig. S8).

### Experimental warming increases transcript abundance from alternative cyanobacteria members, signaling possible symbiont exchange

Differences in the composition and abundance of *Sphagnum*-associated cyanobacteria in response to warming are important because these organisms are some of the key symbionts with

*Sphagnum* mosses (Granhall & Hofsten, 1976), and the exchange of symbionts with more thermotolerant forms have been implicated in host thermotolerance in other systems (Rodriguez *et al.*, 2008). To explore this further, we taxonomically refined three of our high-quality cyanobacteria MAGs with a phylogenetic tree reconstruction using an additional 109 cyanobacterial genomes (Fig. 4). We found that all three cyanobacterial MAGs belong to the heterocystous B1 clade of Cyanobacteria, which also contains known plant associates (Shih *et al.*, 2013). To determine which of the cyanobacteria are most responsive to thermal conditions, we aligned the microbial RNA-seq reads from the end of the experiment onto the MAGs. Of all non-*Sphagnum* RNA-seq reads,  $31.6 \pm 8.7\%$  mapped onto cyanobacteria MAGs for matched ambient-microbiome and ambient temperature conditions. This percentage decreased to  $26.1 \pm 1.1\%$  when plants receiving ambient-microbiomes were subjected to discordant warming treatment. Further, microbiomes originating from warming field conditions contained negligible levels of cyanobacterial RNA-seq reads (0.1–0.08%). Cyanobacterial reads predominantly aligned to MAG bin 14 ( $98 \pm 0.7\%$ ), but to a considerably lesser extent ( $49 \pm 0.6\%$ ) when placed under warming experimental conditions. The decrease in bin 14 RNA-seq reads was accompanied by an increase in reads from Cyanobacteria bin 354 ( $28 \pm 0.6\%$ ) and bin 192 ( $15 \pm 0.9\%$ ) (Fig. 3b). Due to sampling constraints, we did not normalize the results of RNA-seq analysis to community abundance changes.

### Host plant transcriptional response to warming

Given that the warming environment alters community composition in a way that benefits host plant acclimation to warming, we hypothesized that the warming environment selects for more thermotolerant symbionts that are able to maintain nitrogen exchange with the plant at elevated temperatures. If this is the

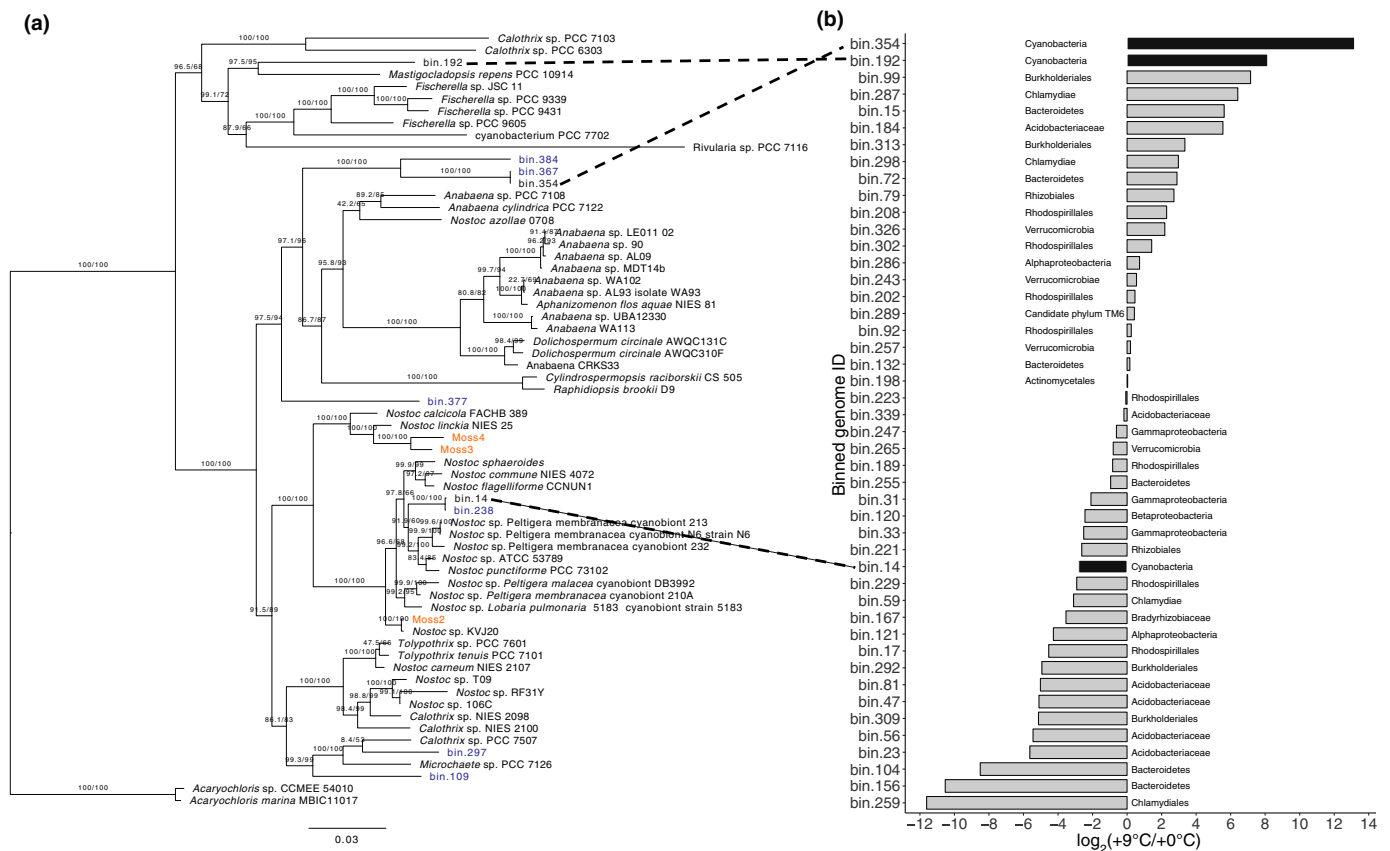


**Fig. 4** Bar chart representing *Cyanobacteria*  $\log_2$ (fold change) of counts per million reads mapping to metagenomic bins between ambient-microbiome and warm-microbiome metagenome samples. Phylogeny of selected *Cyanobacteria* and  $\log_2$ (fold change) of metagenomic bins. (a) Maximum-likelihood phylogram where the numbers at nodes indicate UFB<sub>oot</sub>2 and Shimodaira–Hasegawa-like approximate likelihood ratio support. Branch lengths indicate estimated substitutions per site. Metagenomic bin taxa labels are colored by source from either within peatland responses under changing environments (SPRUCE) (blue) or from Warshan *et al.* (2017) (orange). (b) Bar chart representing  $\log_2$ (fold change) of metagenomic bins between ambient-microbiome and warm-microbiome metagenomes. Black bars indicate cyanobacterial metagenome-assembled genomes (MAGs) recovered in this work.

case, we would expect that plant and microbial transcriptional patterns relating to N transport and metabolism would be similar between matched origin and temperature conditions (i.e. warm-microbiome + warming treatment or ambient-microbiome + ambient treatment). Functional ontology enrichment analysis across all conditions revealed that in plants receiving an ambient-microbiome and ambient treatment, gene expression was enriched for pathways involved in N metabolism, including ammonium transporters, ammonium assimilation and glutamine synthetase, as well as growth-related ontologies including photosynthesis, cytoskeletal elongation and hormonal regulation (Fig. 5a). This was also apparent on an LFC basis when comparing plants with an ambient-microbiome between temperature conditions (Dataset S1). In this case, ambient treatment plants corroborated enrichment analysis with induced ammonium transport (LFC 4.0,  $P=2.0 \times 10^{-2}$ ) and glutamine synthetase (LFC 2.4,  $P=1.1 \times 10^{-2}$ ). In addition, 153 of 178 genes within the photosynthesis ontology were induced, with PSII light-harvesting complex II most strongly affected (LFC 2.1,  $P=2.48 \times 10^{-6}$ ). In addition, we noted differences in fatty acid synthesis, especially in desaturation and elongation (LFC 2.74,  $P=2.97 \times 10^{-6}$ ), phenolic secondary metabolite production

(LFC 2.86,  $P=1.77 \times 10^{-5}$ ), cell wall expansion (LFC 6.5,  $P=2.7 \times 10^{-6}$ ), phytohormone signaling with noncysteine-rich peptides (LFC 4.63,  $P=8.1 \times 10^{-4}$ ), jasmonic acid synthesis (LFC 2.36,  $P=4 \times 10^{-2}$ ) and response to external stimuli (LFC 2.53,  $P=3.2 \times 10^{-2}$ ). As expected, heat shock proteins (HSPs) were responsive to warming, especially the HSP70 family, of which 15 members were induced (LFC 1.2,  $P=6.5 \times 10^{-3}$ ).

Plant ontology enrichment analysis did not support the hypothesis that the warm-microbiome would provision the plant with N at warming treatment conditions (Fig. 5a). Likewise, there was no support for this hypothesis on an LFC basis when comparing RNA-seq profiles from plants with warm-microbiomes across temperature treatments (Dataset S1). Despite the apparent lack of microbially provided fixed N, the warm-microbiome still provided growth benefits to warming-treated plants (Fig. 1b), and this was also apparent in RNA-seq enrichment analysis of growth-related ontologies. Specifically, plants exposed to warming that received warm-microbiomes exhibited enrichment for photosynthesis – PSII light harvesting complex II (LFC 1.4,  $P=1.9 \times 10^{-3}$ ), cell wall expansion (LFC 2.5,  $P=1.3 \times 10^{-5}$ ) and phenolic secondary metabolite production (LFC 2.9,  $P=2.0 \times 10^{-8}$ ).



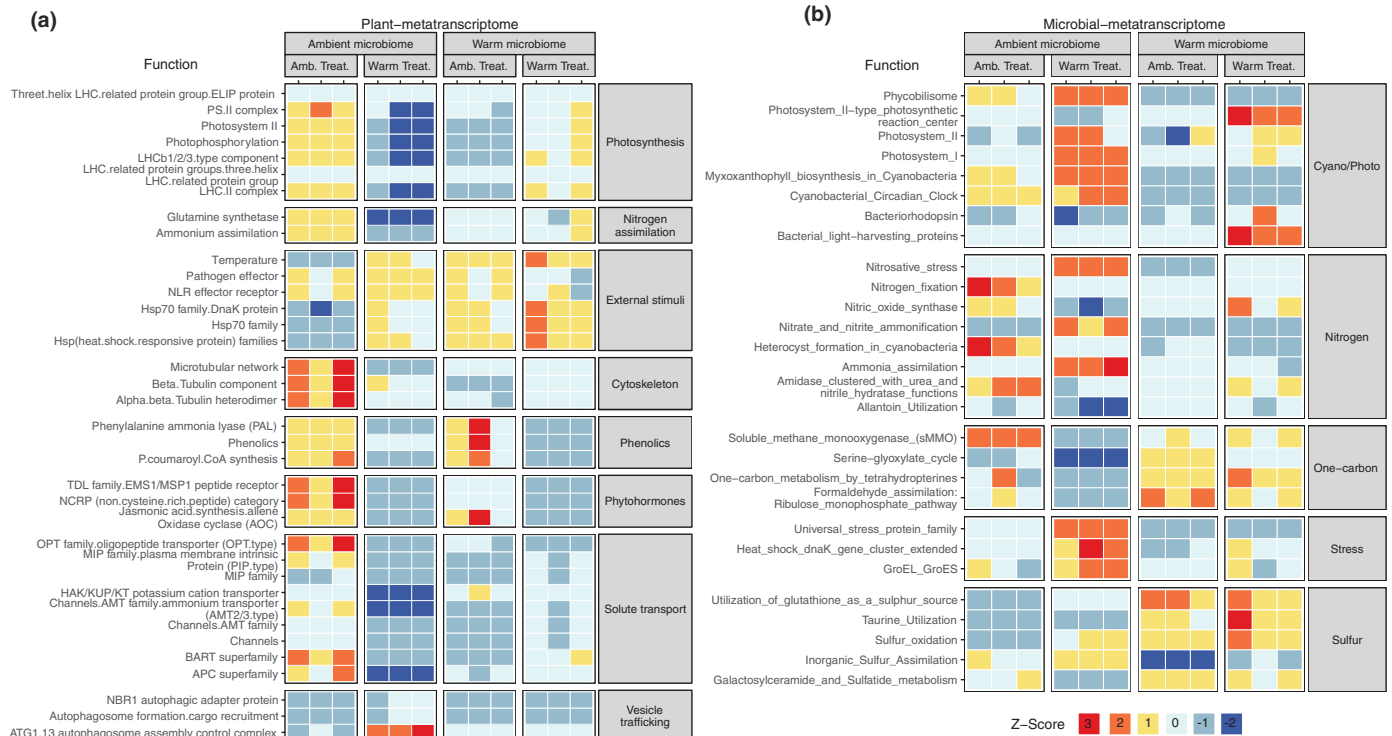


**Fig. 5** Plant and microbial ontology enrichment analysis. Heatmap of z-scores for (a) MAPMAN4 ontology categories enriched in differentially expressed *Sphagnum angustifolium* genes and (b) differentially expressed SEED level 3 categories related to nitrogen, one-carbon and sulfur metabolism; cyanobacterial/photosynthesis; and stress. Differential expression was defined as  $|\log_2(\text{fold change})| > 1$  and corrected  $P < 0.05$ .

Microbial RNA-seq DE analysis of functional ontologies supported the notion that the warming-altered cyanobacteria community is not fixing N, and is therefore not provisioning the plant with N. DE enrichment analysis revealed that microbial N metabolism differed dramatically between both treatments and origins (Fig. 5b; Table S14). Indeed, exposure to warming decreased N-fixation ontology gene expression by 53.4-fold (Fig. 5b; Table S13). Moreover, there was no enrichment evidence for N-fixation among the warm-microbiomes, regardless of temperature treatment. This was also apparent with LFC when comparing microbes from a warm-microbiome to those from an ambient-microbiome under ambient treatment conditions where genes enriched for N-fixation substantially decreased (LFC  $-8.0$ ,  $P = 1.6 \times 10^{-9}$ ) (Dataset S2). The same conditions also showed an increase in sulfur-related metabolism via taurine utilization (LFC 1.5,  $P = 2.0 \times 10^{-4}$ ) and the utilization of glutathione as a sulfur source (LFC 2.7,  $P = 1.8 \times 10^{-7}$ ). Although we could not obtain direct evidence for N-fixation in this study due to sample size restrictions, these observations corroborate previous  $^{15}\text{N}_2$ -based fixation rates reported at the same field site where our warm- and ambient-inocula were obtained (Carrell *et al.*, 2019).

How the warm-microbiome influences host plant photosynthesis and growth temperature acclimation remains to be elucidated, but we can glean clues from communities composed of discordant warm-microbes at ambient experimental temperatures. In that case, enrichment for the HSP70 family is induced without heat (Fig. 5a). This trend was also observed

on an LFC basis where 33 out of 35 detected HSPs were induced (Dataset S1).

## Discussion

The establishment of constructed communities derived from microbiome transfers, coupled with comparative metatranscriptomics, revealed several novel aspects of microbial contributions to plant temperature response. First, plants receiving a microbiome from a high-temperature environment exhibited enhanced photosynthetic and growth acclimation responses to similarly warm environments. Second, the warm-microbiome was less diverse than the ambient-microbiome, but contained transcripts from a more diverse set of cyanobacteria, suggesting symbiont swapping or replacement. Finally, the warm-microbiome transferred a thermotolerant phenotype to the plant through host transcriptional reprogramming involving heat shock response and hormonal regulation genes.

Our results demonstrate that the originating thermal habitat of the microbiome has a dramatic effect on *Sphagnum* host acclimation to elevated temperatures. These results were consistent across two years of field-collected donor inocula and two independent laboratory experiments. Although the fact that plants benefit from microbial relationships is well known, the transfer of microbially acquired habitat-specific abiotic stress tolerance to recipient plants was reported much more recently, and to date has largely been limited to endophytic fungi (e.g. Giauque & Hawkes, 2013; Giauque *et al.*, 2019). In an early example of this, Redman *et al.*

(2002) collected a native North American grass, *Dichanthelium lanuginosum*, endemic to geothermal sites with soil temperatures reaching up to 50°C. After isolation of a *Curvularia* sp. fungus and reinoculation onto endophyte-free plants, thermotolerance was conferred to the recipient plant host. This approach of isolating endophytic fungi from plants endemic to extreme habitats in an attempt to confer habitat-associated benefits has been tested a number of times with both successful (Rodriguez *et al.*, 2008; Redman *et al.*, 2011) and mixed results (Giauque & Hawkes, 2013; Giauque *et al.*, 2019). In all cases, the microbial component focused on fungi and was constrained to single-member strain-based studies.

The microbiome transfer approach used in this study allowed us to test habitat-associated benefits from a broader set of organisms that is more representative of the dynamic coevolving community. However, this strategy made it difficult to relate specific taxa to recipient host benefits. For example, the warm-inocula differed substantially between years, even at the phylum level, yet both showed trends in providing host thermal benefits. This is consistent with the idea that microbial community taxonomic composition is not necessarily a clear indication of community function. Indeed, functional similarity independent of taxonomic group has been reported in other systems, including human gut (Moya & Ferrer, 2016) and microalgae (Burke *et al.*, 2011) microbiomes. Hence, the challenge is to look beyond taxonomic association and determine what components of the microbiome are responsible for conferring thermotolerance on the host plant.

One possible mechanism for enhanced host temperature tolerance is the replacement of primary symbionts with more thermotolerant symbionts. *Sphagnum* mosses have long been known to host N<sub>2</sub>-fixing Cyanobacteria as symbionts (Granhall & Hofsten, 1976; Basilier *et al.*, 1978; Basilier, 1979, 1980). More recently, they have been shown to associate with a suite of bacteria, including those that oxidize methane into CO<sub>2</sub>, as well as a number of viral, archaea and protists (reviewed by Kostka *et al.*, 2016). The influence of warming on these symbionts, especially the Cyanobacteria, would directly affect host nutrient status and productivity. Our metagenome analysis assembled three cyanobacterial MAGs. DNA and RNA-seq reads mapping to the binned MAG genomes indicated that *Sphagnum* plants were primarily colonized by a single cyanobacterial member from the genus *Nostoc*. With increasing temperature, this *Nostoc* MAG decreased in abundance, while two additional cyanobacterial MAGs increased in abundance, indicating a possible exchange for more thermotolerant members of the clade. Precedent for symbiont shuffling has been provided in coral systems. Corals host algal symbiont communities that are genetically diverse and susceptible to symbiont loss due to environmental stress and ensuing coral bleaching events. However, the stress events leading to the bleaching, as well as the bleaching itself, provide an opportunity for replacement of symbionts with organisms that are more suitable to the new environmental condition, such as those with higher stress tolerance (reviewed by Apprill, 2020). The coral system also demonstrates the potential role of the surrounding bacterial community in coral thermotolerance. This was elegantly demonstrated by Ziegler *et al.* (2017), who showed that long-term

temperature elevation modified the composition of the bacterial community, and that particular bacterial taxa could predict coral thermotolerance. However, the coral system is not amenable to germ-free host strains or microbiome transfers, making it difficult to quantify the contribution of the microbiome to host thermotolerance.

From the results of this study, it is difficult to discern whether host thermal benefits from the donor microbiome are driven by community change from primary *Nostoc* cyanobacterial symbionts, or instead by the surrounding microbial community. Our hypothesis that the key cyanobacterial symbiont was augmented by additional thermotolerant cyanobacteria to maintain N<sub>2</sub> fixation at elevated temperatures was not entirely supported. Although we observed an increase in cyanobacteria diversity and ontology enrichment for photosynthesis, thereby providing support for exchange with thermotolerant symbionts, the metatranscriptome analysis yielded no evidence for N<sub>2</sub>-fixation under warming. Caution must be observed as evidence for N<sub>2</sub>-fixation in the current study is based on gene transcriptional analysis and not direct measures for <sup>15</sup>N<sub>2</sub> incorporation. However, this finding is consistent with a previous field study (Carrell *et al.*, 2019) at the same SPRUCE site, where 16S rDNA amplicon profiling, *nifH* quantitative reverse transcriptase PCR and <sup>15</sup>N<sub>2</sub> incubation assays revealed a decrease in *nifH*-containing N-fixing bacteria and a reduction in <sup>15</sup>N<sub>2</sub> incorporation in response to warming.

In addition to N metabolism, recent studies have identified a role for sulfur exchange within feathermoss – and *Sphagnum* – cyanobacterial symbioses (Warshan *et al.*, 2017; Stuart *et al.*, 2020; Carrell *et al.*, 2021). For example, Stuart *et al.* (2020) found that targeted mutagenesis of the cyanobacterial alkane sulfonate monooxygenase resulted in an inability to colonize feathermoss. In addition, Carrell *et al.* (2021) used metabolic cross-feeding and spatial metabolite profiling to discover that *Sphagnum* provided sulfur-rich choline-*O*-sulfate, taurine and sulfoacetate, which were subsequently depleted by the *Nostoc* symbiont. Within the current study, the warm-microbiome showed enrichment for bacterially related sulfur metabolism regardless of treatment temperature. Whether bacterial sulfur metabolism is specific to the cyanobacterial component of the microbiome and the role sulfur metabolism plays in *Sphagnum*-microbiome functioning remains to be elucidated.

Despite the lack of evidence for microbial N<sub>2</sub>-fixation in contributing to plant thermotolerance, the metatranscriptome analysis did reveal a role for heat shock and hormonal reprogramming as potential host pathways underlying the microbial transfer of thermotolerance. Multiple studies have shown that insertional mutants or antisense transgenics for HSP70 fail to acquire thermotolerance, while the overexpression of HSP70 seems to enhance thermotolerance (Larkindale *et al.*, 2007). Within the model plant *Arabidopsis thaliana*, the HSP70s represent a multi-gene family whose proteins are found within all subcellular compartments of the cell where they can refold stress-denatured proteins and prevent aggregation of denatured proteins (Sung *et al.*, 2001). Within the current study, plants grown at ambient temperatures were enriched for Hsp70 gene family transcripts when they received a warm-microbiome, but not when they

received an ambient-microbiome. Shekhawat *et al.* (2021) also observed an increase in HSP70 gene expression in *Arabidopsis* and wheat plants when colonized by the *Enterobacter* sp. root endophyte, yet this was only observed under heat stress and not ambient temperature conditions. Furthermore, our metatranscriptome analysis did not show microbial-mediated repression of the Hsp90 family or induction of the Hsp101 family, both of which have been implicated in the heat shock response. While microbially mediated repression of *Arabidopsis* Hsp90, leading to elevated thermotolerance, was previously demonstrated in the desert-dwelling fungus *Paraphaeosphaeria quadrisepitata* (McLellan *et al.*, 2007), results from the current study only show a role for HSP70s.

In addition to HSP70 reprogramming, microbial thermotolerance may have been transferred via hormonal pathways. The warm-microbiome elicited host plant expression of genes contributing to jasmonic acid synthesis (via allene oxide cyclase (AOC)). Jasmonic acid is a key phytohormone contributing to both abiotic and biotic stress responses, and has been implicated in flowering plant thermotolerance (Clarke *et al.*, 2009). AOC synthesizes 12-oxo-phytodienoic acid (OPDA), which is a signaling compound and intermediate in the jasmonic acid biosynthesis pathway. In the liverwort *Marchantia polymorpha*, overexpression of AOC increases OPDA, suggesting that its function is similar to that of its homologs in flowering plants (Yamamoto *et al.*, 2015). However, AOC overexpression in *M. polymorpha* decreases growth. Likewise, the warm-microbiome induced expression of enzymes involved in the production of phenolic compounds, including phenylalanine ammonia lyase (PAL), which has been implicated in both temperature response and disease resistance (Huang *et al.*, 2010). In contrast to the heat shock response, the jasmonic acid and phenolic ontology enrichments disappeared after the plants were exposed to warming. Furthermore, the ambient-microbiome elicited some aspects of jasmonic acid synthesis as well indicating that more research is needed to determine if cross-talk with the heat shock response occurs. Thus, it remains to be determined whether these compounds are contributing to a beneficial thermal preconditioning or instead reflect a defensive response.

One unexpected observation was that the warm-microbiome elicited the induction of the heat shock response in plants that were never exposed to elevated temperatures. Thermotolerance can be acquired by previous exposure to a sublethal temperature stress (Kotak *et al.*, 2007). Similarly, plants associated with beneficial rhizosphere microbes can more rapidly mount a defense response to biotic and abiotic stressors (Conrath *et al.*, 2006). Although there is a considerable body of literature on the biotic aspects of microbially induced plant priming, increasing evidence suggests that plants can also be primed against abiotic stressors. For example, Ali *et al.* (2009) found that a *Pseudomonas* sp. strain isolated from pigeon pea endemic to an arid region conferred enhanced survival and growth on sorghum seedlings exposed to elevated temperatures. This early example has been corroborated with multiple plant hosts and microbial strains, yet the underlying genetic mechanisms remain to be identified (Yamamoto *et al.*, 2015). In most cases studied thus

far, microbially induced resistance to abiotic stress has been studied in individual strains or small community consortia. By contrast, in this study we examined how microbial dynamics within more complex communities interact to influence host physiology and growth.

## Conclusions

Our findings provide a starting point for future studies that systematically decouple inherent host acclimation responses to challenging environmental conditions from those of the associated microbiome. A key benefit of the microbiome transfer and constructed community approaches described here is that they allow the coevolved host–microbiome consortia collected from extreme environmental conditions to be separated and tested across a range of thermal experimental conditions. Our observation that the microbiome can transmit thermotolerant phenotypes has a number of implications. It sets the stage for moving beyond the current notion that plants are restricted to ‘adapt or migrate’ strategies for survival to rapidly changing environmental conditions (Lau & Lennon, 2012). The current study provides an alternative perspective on these outcomes by showing that thermotolerant phenotypes can be rapidly transmitted to plant hosts. We anticipate multiple challenges as the findings of our studies are transferred beyond the laboratory into ecological systems. First, additional research is needed to determine the extent to which inter- and intraspecific genetic variation influences the plant’s ability to receive microbial benefits, and if so, to identify the causal alleles. Bringing this goal closer to reality, a genome sequencing campaign representing some 78 species within the *c.* 300-member genus *Sphagnum*, as well as the development of high-density genetic maps from sequencing of a 200-member pedigree cross, are currently underway (Weston *et al.*, 2018). Second, the identification of responsible microbial taxa is challenged by large community diversity, complex community interactions and strain isolation limitations. These experimental tests could take multiple forms, including the dilution and sequencing of donor microbiomes or strain isolation and testing in our demonstrated plate-based experimental system or repeat transfers of field conditioned microbiomes paired with isotope tracing and metatranscriptomics. Within the context of this study, such an approach could determine whether microbial benefits are mainly a function of swapping primary cyanobacteria symbionts for more thermotolerant members, or whether additional microbial members are driving the host phenotype. In closing, the current study revealed that warming altered microbial community structure in a manner that induced the plant heat shock response, especially the HSP70 family and jasmonic acid production. Hsp70 induction occurred even without a warming treatment, suggesting that the warm-microbiome itself can induce plant thermal acclimation.

## Acknowledgements













We are grateful for the editor and reviewers for detailed and constructive comments, presubmission comments from Dr Gustaf

Granath and field site maintenance from Robert Nettles III. Collection of starting microbial inocula was made possible through the SPRUCE project, which is supported by the Office of Science; Biological and Environmental Research (BER); US Department of Energy (DOE), grant/award no. DE-AC05-00OR22725. Experimentation, sample collection and analyses were supported by the DOE BER Early Career Research Program. Oak Ridge National Laboratory is managed by UT-Battelle, LLC, for the US DOE under contract no. DE-AC05-00OR22725. AJS was supported by NSF DEB-1737899, 1928514. The work conducted by the US DOE Joint Genome Institute (JGI) is supported by the Office of Science of the US Department of Energy under contract no. DE-AC02-05CH11231. We thank the DOE JGI and collaborators for pre-publication access to the *S. angustifolium* (formerly *S. fallax*) genome sequence.

### Author contributions

AAC and DJW designed research; AAC, TJL, DJW, DAP, SSJ and JG performed research; AAC, TJL, KGMC and DLC analyzed data; JS, PJH, AJS, AAC, TJL, DJW, DAP, DLC, KGMC and JHL wrote the manuscript.

### ORCID

Kristine Grace M. Cabugao  <https://orcid.org/0000-0002-1024-192X>  
 Dana L. Carper  <https://orcid.org/0000-0002-4758-8054>  
 Alyssa A. Carrell  <https://orcid.org/0000-0003-1142-4709>  
 Jane Grimwood  <https://orcid.org/0000-0002-8356-8325>  
 Paul J. Hanson  <https://orcid.org/0000-0001-7293-3561>  
 Sara S. Jawdy  <https://orcid.org/0000-0002-8123-5439>  
 Travis J. Lawrence  <https://orcid.org/0000-0002-7380-489X>  
 Jun Hyung Lee  <https://orcid.org/0000-0002-7137-7169>  
 Dale A. Pelletier  <https://orcid.org/0000-0002-4321-7918>  
 Jeremy Schmutz  <https://orcid.org/0000-0001-8062-9172>  
 A. Jonathan Shaw  <https://orcid.org/0000-0002-7344-9955>  
 David J. Weston  <https://orcid.org/0000-0002-4794-9913>

### Data availability

Raw 16S and ITS sequence files can be found on NCBI using the BioProject ID PRJNA644113. Raw metagenome and metatranscriptome sequence files can be found on NCBI using the BioProject ID PRJNA644538.

### References

- Ali SZ, Sandhya V, Grover M, Kishore N, Rao LV, Venkateswarlu B. 2009. *Pseudomonas* sp. strain AKM-P6 enhances tolerance of sorghum seedlings to elevated temperatures. *Biology and Fertility of Soils* 46: 45–55.
- Apprill A. 2020. The role of symbioses in the adaptation and stress responses of marine organisms. *Annual Review of Marine Science* 12: 291–314.
- Baker DM, Freeman CJ, Wong JCY, Fogel ML, Knowlton N. 2018. Climate change promotes parasitism in a coral symbiosis. *ISME Journal* 12: 921–930.
- Basilier K. 1979. Moss-associated nitrogen fixation in some mire and coniferous forest environments around Uppsala, Sweden. *Lindbergia* 5: 84–88.
- Basilier K. 1980. Fixation and uptake of nitrogen in sphagnum blue-green algal associations. *Oikos* 34: 239–242.
- Basilier K, Granhall U, Stenström T-A, Stenstrom T-A. 1978. Nitrogen fixation in wet minerotrophic moss communities of a subarctic mire. *Oikos* 31: 236–246.
- Basińska AM, Reczuga MK, Gąbka M, Stróżecki M, Łuców D, Samson M, Urbaniak M, Leśny J, Chojnicki BH, Gilbert D *et al.* 2020. Experimental warming and precipitation reduction affect the biomass of microbial communities in a Sphagnum peatland. *Ecological Indicators* 112: 106059.
- Bay LK, Doyle J, Logan M, Berkelmans R, Bay LK. 2016. Recovery from bleaching is mediated by threshold densities of background thermo-tolerant symbiont types in a reef-building coral. *Royal Society Open Science* 3: 160322.
- Berg A, Danielsson Å, Svensson BH. 2013. Transfer of fixed-N from N<sub>2</sub>-fixing cyanobacteria associated with the moss *Sphagnum riparium* results in enhanced growth of the moss. *Plant and Soil* 362: 271–278.
- Bolyen E, Rideout JR, Dillon MR, Bokulich NA, Abnet CC, Al-Ghalith GA, Alexander H, Alm EJ, Arumugam M, Asnicar F *et al.* 2019. Reproducible, interactive, scalable and extensible microbiome data science using QIIME 2. *Nature Biotechnology* 37: 852–857.
- Bowers RM, Kyrpides NC, Stepanauskas R, Harmon-Smith M, Doud D, Reddy TBK, Schulz F, Jarett J, Rivers AR, Eloie-Fadrosch EA *et al.* 2017. Minimum information about a single amplified genome (MISAG) and a metagenome-assembled genome (MIMAG) of bacteria and archaea. *Nature Biotechnology* 35: 725–731.
- Bragazza L. 2008. A climatic threshold triggers the die-off of peat mosses during an extreme heat wave. *Global Change Biology* 14: 2688–2695.
- Bragazza L, Buttler A, Robroek BJM, Albrecht R, Zaccane C, Jassey VEJ, Signarbieux C. 2016. Persistent high temperature and low precipitation reduce peat carbon accumulation. *Global Change Biology* 22: 4114–4123.
- van Breemen N. 1995. How *Sphagnum* bogs down other plants. *Trends in Ecology & Evolution* 10: 270–275.
- Buchfink B, Xie C, Huson DH. 2014. Fast and sensitive protein alignment using DIAMOND. *Nature Methods* 12: 59–60.
- Burke C, Steinberg P, Rusch D, Kjelleberg S, Thomas T. 2011. Bacterial community assembly based on functional genes rather than species. *Proceedings of the National Academy of Sciences, USA* 108: 14288–14293.
- Callahan BJ, McMurdie PJ, Rosen MJ, Han AW, Johnson AJ, Holmes SP. 2016. DADA2: high-resolution sample inference from Illumina amplicon data. *Nature Methods* 13: 581–583.
- Carrell AA, Kolton M, Glass JB, Pelletier DA, Warren MJ, Kostka JE, Iversen CM, Hanson PJ, Weston DJ. 2019. Experimental warming alters the community composition, diversity, and N<sub>2</sub> fixation activity of peat moss (*Sphagnum fallax*) microbiomes. *Global Change Biology* 25: 2993–3004.
- Carrell AA, Velicković D, Lawrence TJ, Bowen BP, Louie KB, Carper DL, Chu RK, Mitchell HD, Orr G, Markillie LM *et al.* 2021. Novel metabolic interactions and environmental conditions mediate the boreal peatmoss-cyanobacteria mutualism. *ISME Journal* 29: 1–2.
- Clarke SM, Cristescu SM, Miersch O, Harren FJM, Wasternack C, Mur LAJ. 2009. Jasmonates act with salicylic acid to confer basal thermotolerance in *Arabidopsis thaliana*. *New Phytologist* 182: 175–187.
- Clymo RS, Hayward PM. 1982. The ecology of *Sphagnum*. In: Smithn AJE, ed. *Bryophyte ecology*. Dordrecht, the Netherlands: Springer, 229–289.
- Conrath U, Beckers GJM, Flors V, García-Agustín P, Jakob G, Mauch F, Newman M-A, Pieterse CMJ, Poinssot B, Pozo MJ *et al.* 2006. Priming: getting ready for battle. *Molecular Plant–Microbe Interactions* 19: 1062–1071.
- Cregger MA, Veach AM, Yang ZK, Crouch MJ, Vilgalys R, Tuskan GA, Schadt CW. 2018. The *Populus* holobiont: dissecting the effects of plant niches and genotype on the microbiome. *Microbiome* 6: 1–4.
- Cunning R, Silverstein RN, Baker AC. 2015. Investigating the causes and consequences of symbiont shuffling in a multi-partner reef coral symbiosis under environmental change. *Proceedings of the Royal Society B: Biological Sciences* 282: 20141725.
- Fox J, Weisberg S. 2018. *An R companion to applied regression*. New York, NY, USA: Sage Publications.

- Giaouque H, Connor EW, Hawkes CV. 2019. Endophyte traits relevant to stress tolerance, resource use and habitat of origin predict effects on host plants. *New Phytologist* 221: 2239–2249.
- Giaouque H, Hawkes CV. 2013. Climate affects symbiotic fungal endophyte diversity and performance. *American Journal of Botany* 100: 1435–1444.
- Gorham E. 1991. Northern peatlands: role in the carbon cycle and probable responses to climatic warming. *Ecological Applications* 1: 182–195.
- Granhall ULF, Hofsten AV. 1976. Nitrogenase activity in relation to intracellular organisms in *Sphagnum* mosses. *Physiologia Plantarum* 36: 88–94.
- Gunnarsson U, Granberg G, Nilsson M. 2004. Growth, production and interspecific competition in *Sphagnum*: effects of temperature, nitrogen and sulphur treatments on a boreal mire. *New Phytologist* 163: 349–359.
- Hanson PJ, Gill AL, Xu X, Phillips JR, Weston DJ, Kolka RK, Riggs JS, Hook LA. 2016. Intermediate-scale community-level flux of CO<sub>2</sub> and CH<sub>4</sub> in a Minnesota peatland: putting the SPRUCE project in a global context. *Biogeochemistry* 129: 255–272.
- Heath KD, Stock AJ, Stinchcombe JR. 2010. Mutualism variation in the nodulation response to nitrate. *Journal of Evolutionary Biology* 23: 2494–2500.
- Heck MA, Lüth VM, van Gessel N, Krebs M, Kohl M, Prager A, Joosten H, Decker EL, Reski R. 2021. Axenic in vitro cultivation of 19 peat moss (*Sphagnum* L.) species as a resource for basic biology, biotechnology, and paludiculture. *New Phytologist* 229: 861–876.
- Howles EJ, Abrego D, Meyer E, Kirk NL, Burt JA. 2016. Host adaptation and unexpected symbiont partners enable reef-building corals to tolerate extreme temperatures. *Global Change Biology* 22: 2702–2714.
- Huang J, Gu M, Lai Z, Fan B, Shi K, Zhou YH, Yu JQ, Chen Z. 2010. Functional analysis of the Arabidopsis *PAL* gene family in plant growth, development, and response to environmental stress. *Plant Physiology* 153: 1526–1538.
- Hupperts SF, Gerber S, Nilsson MC, Gundale MJ. 2021. Empirical and Earth system model estimates of boreal nitrogen fixation often differ: a pathway toward reconciliation. *Global Change Biology* 27: 5711–5725.
- Jassey VEJ, Signarbieux C, Hättenschwiler S, Bragazza L, Buttler A, Delarue F, Fournier B, Gilbert D, Laggoun-Défarge F, Lara E *et al.* 2015. An unexpected role for mixotrophs in the response of peatland carbon cycling to climate warming. *Scientific Reports* 5: 1–10.
- Kip N, van Winden JF, Pan Y, Bodrossy L, Reichart G-J, Smolders AJP, Jetten MSM, Damsté JSS, Op den Camp HJM. 2010. Global prevalence of methane oxidation by symbiotic bacteria in peat-moss ecosystems. *Nature Geoscience* 3: 617–621.
- Kostka JE, Weston DJ, Glass JB, Lilleskov EA, Shaw AJ, Turetsky MR. 2016. The *Sphagnum* microbiome: new insights from an ancient plant lineage. *New Phytologist* 211: 57–64.
- Kotak S, Larkindale J, Lee U, von Koskull-Döring P, Vierling E, Scharf KD. 2007. Complexity of the heat stress response in plants. *Current Opinion in Plant Biology* 10: 310–316.
- Lamentowicz M, Mitchell EAD. 2005. The ecology of testate amoebae (protists) in *Sphagnum* in north-western Poland in relation to peatland ecology. *Microbial Ecology* 50: 48–63.
- Larkindale J, Mishkind M, Vierling E. 2007. Plant responses to high temperature. *Plant Abiotic Stress* 100: 144.
- Larmoia T, Leppanen SM, Tuittila ES, Aarva M, Merila P, Fritze H, Tirola M. 2014. Methanotrophy induces nitrogen fixation during peatland development. *Proceedings of the National Academy of Sciences, USA* 111: 734–739.
- Lau JA, Lennon JT. 2012. Microbe-mediated adaptation to novel environments. *Proceedings of the National Academy of Sciences, USA* 109: 14058–14062.
- Liao Y, Smyth GK, Shi W. 2019. The R package Rsubread is easier, faster, cheaper and better for alignment and quantification of RNA sequencing reads. *Nucleic Acids Research* 47: e47.
- Liebner S, Svenning MM. 2013. Environmental transcription of *mmoX* by methane-oxidizing *Proteobacteria* in a subarctic peatland. *Applied and Environmental Microbiology* 79: 701–706.
- Lindo Z, Nilsson MC, Gundale MJ. 2013. Bryophyte-cyanobacteria associations as regulators of the northern latitude carbon balance in response to global change. *Global Change Biology* 19: 2022–2035.
- McLellan CA, Turbyville TJ, Kithsiri Wijeratne EM, Kerschen A, Vierling E, Queitsch C, Whitesell L, Gunatilaka AAL. 2007. A rhizosphere fungus enhances *Arabidopsis* thermotolerance through production of an *HSP90* inhibitor. *Plant Physiology* 145: 174–182.
- McMurdie PJ, Holmes S. 2013. PHYLOSEQ: an R package for reproducible interactive analysis and graphics of microbiome census data. *PLoS ONE* 8: e61217.
- Moya A, Ferrer M. 2016. Functional redundancy-induced stability of gut microbiota subjected to disturbance. *Trends in Microbiology* 24: 402–413.
- Norby RJ, Childs J, Hanson PJ, Warren JM. 2019. Rapid loss of an ecosystem engineer: *Sphagnum* decline in an experimentally warmed bog. *Ecology and Evolution* 9: 12571–12585.
- Overbeek R, Olson R, Pusch GD, Olsen GJ, Davis JJ, Disz T, Edwards RA, Gerdes S, Parrello B, Shukla M *et al.* 2014. The SEED and the rapid annotation of microbial genomes using subsystems technology (RAST). *Nucleic Acids Research* 42: D206–D214.
- Parks DH, Imelfort M, Skennerton CT, Hugenholtz P, Tyson GW. 2015. CheckM: assessing the quality of microbial genomes recovered from isolates, single cells, and metagenomes. *Genome Research* 25: 1043–1055.
- R Core Team. 2021. *R: a language and environment for statistical computing, v.3.6.1, R 4.1*. Vienna, Austria: R Foundation for Statistical Computing. [WWW document] URL <https://www.R-project.org/> [accessed 1 August 2021].
- Raghoebarsing AA, Smolders AJP, Schmid MC, Rijpstra WIC, Wolters-Arts M, Derksen J, Jetten MSM, Schouten S, Sinninghe Damsté JS, Lamers LPM *et al.* 2005. Methanotrophic symbionts provide carbon for photosynthesis in peat bogs. *Nature* 436: 1153–1156.
- Reczuga MK, Seppey CVW, Mulot M, Jassey VEJ, Buttler A, Słowińska S, Słowiński M, Lara E, Lamentowicz M, Mitchell EAD. 2020. Assessing the responses of *Sphagnum* micro-eukaryotes to climate changes using high throughput sequencing. *PeerJ* 8: e9821.
- Redman RS, Kim YO, Woodward CJDA, Greer C, Espino L, Doty SL, Rodriguez RJ. 2011. Increased fitness of rice plants to abiotic stress via habitat adapted symbiosis: a strategy for mitigating impacts of climate change. *PLoS ONE* 6: 1–10.
- Redman RS, Sheehan KB, Stout RG, Rodriguez RJ, Henson JM. 2002. Thermotolerance generated by plant/fungal symbiosis. *Science* 298: 1581.
- Ritchie ME, Phipson B, Wu DI, Hu Y, Law CW, Shi W, Smyth GK. 2015. limma powers differential expression analyses for RNA-sequencing and microarray studies. *Nucleic Acids Research* 43: e47.
- Robroek BJM, Limpens J, Breeuwer A, Crusell PH, Schouten MGC. 2007a. Interspecific competition between *Sphagnum* mosses at different water tables. *Functional Ecology* 21: 805–812.
- Robroek BJM, Limpens J, Breeuwer A, Schouten MGC. 2007b. Effects of water level and temperature on performance of four *Sphagnum* mosses. *Plant Ecology* 190: 97–107.
- Rodriguez RJ, Henson J, Van Volkenburgh E, Hoy M, Wright L, Beckwith F, Kim Y-O, Redman RS. 2008. Stress tolerance in plants via habitat-adapted symbiosis. *ISME Journal* 2: 404–416.
- Schneider CA, Rasband WS, Eliceiri KW. 2012. NIH image to ImageJ: 25 years of image analysis. *Nature Methods* 9: 671–675.
- Schwacke R, Ponce-Soto GY, Krause K, Bolger AM, Arsova B, Hallab A, Gruden K, Stitt M, Bolger ME, Usadel B. 2019. MapMan4: a refined protein classification and annotation framework applicable to multi-omics data analysis. *Molecular Plant* 12: 879–892.
- Shekhawat K, Saad MM, Sheikh A, Mariappan K, Al-Mahmoudi H, Abdulhakim F, Eida AA, Jalal R, Masmoudi K, Hirt H. 2021. Root endophyte induced plant thermotolerance by constitutive chromatin modification at heat stress memory gene loci. *EMBO Reports* 22: e51049.
- Shih PM, Wu D, Latifi A, Axen SD, Fewer DP, Talla E, Calteau A, Cai F, Tandeau de Marsac N, Rippka R *et al.* 2013. Improving the coverage of the cyanobacterial phylum using diversity-driven genome sequencing. *Proceedings of the National Academy of Sciences, USA* 110: 1053–1058.

- Stough JMA, Kolton M, Kostka JE, Weston DJ, Pelletier DA, Wilhelm SW. 2018. Diversity of active viral infections within the *Sphagnum* microbiome. *Applied and Environmental Microbiology* 84: 1–16.
- Stuart RK, Pederson ER, Weyman PD, Weber PK, Rassmussen U, Dupont CL. 2020. Bidirectional C and N transfer and a potential role for sulfur in an epiphytic diazotrophic mutualism. *ISME Journal* 14: 3068–3078.
- Sung DY, Vierling E, Guy CL. 2001. Comprehensive expression profile analysis of the Arabidopsis *Hsp70* gene family. *Plant Physiology* 126: 789–800.
- Thimm O, Blasing O, Gibon Y, Nagel A, Meyer S, Krüger P, Selbig J, Müller LA, Rhee SY, Stitt M. 2014. MAPMAN: a user-driven tool to display genomics data sets onto diagrams of metabolic pathways and other biological processes. *The Plant Journal* 37: 914–939.
- Timm CM, Pelletier DA, Jawdy SS, Gunter LE, Henning JA, Engle N, Aufrecht J, Gee E, Nookaew I, Yang Z *et al.* 2016. Two poplar-associated bacterial isolates induce additive favorable responses in a constructed plant-microbiome system. *Frontiers in Plant Science* 7: 1–10.
- Vile MA, Kelman Wieder R, Živković T, Scott KD, Vitt DH, Hartsock JA, Iosue CL, Quinn JC, Petix M, Fillingim HM *et al.* 2014. N<sub>2</sub> fixation by methanotrophs sustains carbon and nitrogen accumulation in pristine peatlands. *Biogeochemistry* 121: 317–328.
- Warshan D, Espinoza JL, Stuart RK, Richter RA, Kim S-Y, Shapiro N, Woyke T, C Kypides N, Barry K, Singan V *et al.* 2017. Feathermoss and epiphytic *Nostoc* cooperate differently: expanding the spectrum of plant–cyanobacteria symbiosis. *ISME Journal* 11: 2821–2833.
- Weston DJ, Timm CM, Walker AP, Gu L, Muchero W, Schmutz J, Shaw AJ, Tuskan GA, Warren JM, Wulschleger SD. 2014. *Sphagnum* physiology in the context of changing climate: emergent influences of genomics, modelling and host-microbiome interactions on understanding ecosystem function. *Plant, Cell & Environment* 38: 1737–1751.
- Weston DJ, Turetsky MR, Johnson MG, Granath G, Lindo Z, Belyea LR, Rice SK, Hanson DT, Engelhardt KA, Schmutz J *et al.* 2018. The sphagnum project: enabling ecological and evolutionary insights through a genus-level sequencing project. *New Phytologist* 217: 16–25.
- Westreich ST, Korf I, Mills DA, Lemay DG. 2016. SAMSA: a comprehensive metatranscriptome analysis pipeline. *BMC Bioinformatics* 17: 1–2.
- Yamamoto Y, Ohshika J, Takahashi T, Ishizaki K, Kohchi T, Matusuura H, Takahashi K. 2015. Functional analysis of allene oxide cyclase, *MpAOC*, in the liverwort *Marchantia polymorpha*. *Phytochemistry* 116: 48–56.
- Yu Z, Loisel J, Brosseau DP, Beilman DW, Hunt SJ. 2010. Global peatland dynamics since the Last Glacial Maximum. *Geophysical Research Letters* 37: 1–5.
- Ziegler M, Seneca FO, Yum LK, Palumbi SR, Woolstra CR. 2017. Bacterial community dynamics are linked to patterns of coral heat tolerance. *Nature Communications* 8: 1–8.

## Supporting Information

Additional Supporting Information may be found online in the Supporting Information section at the end of the article.

**Dataset S1** Log fold change of RNA-seq profiles from plants with ambient- and warm-microbiomes across temperature treatments and ambient and warming microbiome treatments.

**Dataset S2** Log fold change of RNA-seq profiles from plant microbiomes with ambient and warming microbiomes treatments.

**Fig. S1** Average moss fluorescence in 2016 at the end of the experiment.

**Fig. S2** Average moss fluorescence in 2017 at the end of the experiment.

**Fig. S3** Average moss growth rate under ambient or warming treatments.

**Fig. S4** Bacterial/archaeal amplicon nonmetric multidimensional scaling (NMDS) ordination of the Bray–Curtis distance matrix of inoculum and field.

**Fig. S5** Bacterial/archaeal amplicon nonmetric multidimensional scaling (NMDS) ordination of the Bray–Curtis distance matrix of samples at the end of the experiment.

**Fig. S6** Linear correlation of plant growth rate and fungal (ITS) Shannon diversity at the conclusion of the experiment.

**Fig. S7** Boxplot of percentage of metatranscriptomic reads mapping to *Sphagnum*, metagenome assembly and metagenome assembled genomes.

**Fig. S8** MDS of the top 500 most variable microbial SEED level 3 categories.

**Methods S1** Metagenome sequencing and analysis.

**Table S1** Incubation temperature and light cycle for 2016 and 2017 laboratory experiments.

**Table S2** Summary growth rate and total moss growth over 4 wk.

**Table S3** Two-way ANOVA tables of total moss growth.

**Table S4** Percentage change of total moss growth between microbiome transfers.

**Table S5** Two-way ANOVA tables of moss fluorescence ( $F_v/F_m$ ).

**Table S6** Percentage change of fluorescence at harvest.

**Table S7** Number of paired-end bacterial/archaeal amplicon reads.

**Table S8** Bacterial/archaeal amplicon-based community abundance of starting inoculum.

**Table S9** Bacterial/archaeal amplicon-based community abundance at the end of laboratory incubations.

**Table S10** Fungal amplicon (ITS) phylum-level taxonomy of microbiomes at the end of the laboratory experiment.

**Table S11** Fungal (ITS) class level taxonomy of microbiomes at the end of the laboratory experiment.

**Table S12** Descriptive statistics and log<sub>2</sub> fold change of metagenome assembled genomes (MAG).

**Table S13** Number of paired-end metatranscriptomic reads passing quality control.

**Table S14** Log<sub>2</sub> fold change of SEED subsystem level 3 gene ontologies for the microbial fraction of metatranscriptomic reads.

Please note: Wiley Blackwell are not responsible for the content or functionality of any Supporting Information supplied by the authors. Any queries (other than missing material) should be directed to the *New Phytologist* Central Office.



### About *New Phytologist*

- *New Phytologist* is an electronic (online-only) journal owned by the New Phytologist Foundation, a **not-for-profit organization** dedicated to the promotion of plant science, facilitating projects from symposia to free access for our Tansley reviews and Tansley insights.
- Regular papers, Letters, Viewpoints, Research reviews, Rapid reports and both Modelling/Theory and Methods papers are encouraged. We are committed to rapid processing, from online submission through to publication 'as ready' via *Early View* – our average time to decision is <23 days. There are **no page or colour charges** and a PDF version will be provided for each article.
- The journal is available online at Wiley Online Library. Visit **www.newphytologist.com** to search the articles and register for table of contents email alerts.
- If you have any questions, do get in touch with Central Office (np-centraloffice@lancaster.ac.uk) or, if it is more convenient, our USA Office (np-usaoffice@lancaster.ac.uk)
- For submission instructions, subscription and all the latest information visit **www.newphytologist.com**